ESA Contract

Martian Environment Models

Ref: ESA 11369/95/NL/JG CCN2

WP7.3 deliverable

Technical Report:

CO_2 non-LTE cooling rate at 15-μm and its parameterization for the Mars atmosphere

Miguel A. López-Valverde and Manuel López-Puertas
Instituto de Astrofísica de Andalucía - CSIC, Granada, Spain

March 31, 2001

Contents

Abstract

This report is an IAA contribution to WP7.3 of the ESA Contract Extension 11369/95/NL/JG CCN2, and reviews the investigation of parameterization schemes suitable for implementation of the non-LTE emissions of CO_2 into a general circulation model (GCM).

We first review the different approximations employed in the past in similar problems in the Earth upper atmosphere, as well as the limited number of parameterizations for the Martian case. A simplification exercise is presented that reduces the problem from a full non-LTE reference calculation to increasingly simpler schemes, by imposing a number of approximations, and comparing the results with the full nominal non-LTE cooling rates. A parameterization is then proposed, which is very fast to compute, and is analyzed in the light of current non-LTE uncertainties. The tabulation of the parameters used in the parameterization is included, together with an outline of the steps for its implementation into an operational code. Conclusions and future improvements to the present parameterization are also summarized.

1 Introduction

In a previous report (López-Valverde et al., 1999) we described the basics of the non-LTE problem in the atmosphere of Mars regarding the important infrared bands of CO_2, and the current state of the theoretical models developed in the last years to study them. In the upper atmosphere of Mars those emissions are responsible for important solar heating (from absorptions in the 1-4 μm spectral region, here termed as near-IR) and strong thermal cooling rates (in the broad 15 μm region), and both require a detailed treatment for their inclusion in energy balance studies and circulation models of that atmosphere. However, this is not straightforward given the complexity and non-linearity of the non-LTE situations (see López-Valverde et al. 1999, for more details). Their full simulation requires computational codes which are too expensive for a GCM. Similar problems have been found for CO_2 and other molecular emissions in the Earth's atmosphere.

The problem of the parameterization of the CO_2 solar heating rates in the near-IR in Mars has been tackled recently by López-Valverde et al. (1998) proposing a simple and fast scheme to obtain the non-LTE heating once an LTE calculation is performed. It is implemented as a single profile of correcting factors on a pressure grid, as it was demonstrated that other dependencies are of secondary importance. Unfortunately a similar simple scheme for the thermal cooling rates is not possible because these are strongly affected by the thermal structure as well (López-Puertas and López-Valverde, 1995). The thermal cooling in the 15 μm region requires a more elaborate approach, which is the subject of the current study.

The usual effect of non-LTE on the cooling rates at 15-μm is to reduce them. Under non-LTE the number density of the emitting excited levels is smaller than in LTE because the spontaneous emission to space adds significantly to the collisional relaxations. This is important for the CO_2(0,1,0) state of the major 626 isotope above about 90 km in the Martian atmosphere, and depends non-linearly on the temperature structure and the local absolute value. However, due to radiative transfer, the temperature structure at altitudes one or two scale heights away from this layer can also have profound effects on the cooling (López-Valverde et al., 1998).

Solutions to this problem have been sought in the past following a number of approaches. None of them is, however, very satisfactory for the upper atmosphere of Mars (López-Valverde et al. 1999; see below).

We report here in detail on the research carried out for the development of a new parameterization of the thermal cooling rate due to the 15-μm CO_2 emission bands in the upper atmosphere of Mars. A number of steps were followed during the study, starting from a reference complete calculation. They represent increasing simplifications of the full treatment, and are intended to accelerate the computation of the CO_2 cooling rates while maintaining an acceptable accuracy.

In section 2, we first make a brief revision of the different approaches employed in the case of the Earth's upper atmosphere and of the less studied Martian case. In section 3, we present the strategy followed in this work, explaining the major steps in the simplification process, and the results obtained.

These are analyzed and compared to current uncertainties in non-LTE parameters. The parameterization and the associated tabulation are summarized in section 4. A summary of the work, with a brief discussion of the desired improvements for the future are presented in section 5.

2 Review of fast calculations of non-LTE cooling rates

2.1 Parameterizations in the Earth's atmosphere

Running a non-LTE code on-line within a GCM in order to compute thermal cooling and solar heating rates is completely impractical, as explained above. A number of acceleration methods have been investigated in the past for similar problems in the Earth's atmosphere. These have included simplifications of both the statistical equilibrium equations and the radiative transfer equations.

Regarding the statistical equilibrium equations, the usage of a 2-level system has been the preferred solution for the CO_2 studies. This consists of an excited state in addition to the ground state of the molecule, with V–T collisional excitation and relaxation of the upper state. The non-LTE departure is therefore postulated as the competition between relaxation by collisions versus spontaneous emission. No allowance is made for V–V exchanges; these are of very minor importance for the 15 μm levels of CO_2 in the terrestrial case, although they are of primary importance in Mars (see below).

Regarding the radiative transfer, the different approaches can basically be divided in four techniques, as follows.

(1) A more or less elaborated version of the cool-to-space approximation; this is very fast to implement for an individual CO_2 emission band or for a group of bands. Related versions, also very fast but of validity within very well defined conditions, are the optically thin and the Newtonian cooling approximations.

(2) The usage of broadband models, which do not retain the explicit expression of the heating rate in radiative transfer theory. These have been mainly developed for LTE conditions and very broad spectral regions (not for individual molecular bands, as required in non-LTE, although this should not present any serious limitation).

(3) A tabulation of pre-computed atmospheric transmittances, plus an appropriate interpolation tool; this strategy is more time consuming, but obviously much faster than the actual calculation of transmittances, even if this uses a band model or any accelerated computation of the integrals involved in the heating rate expression of the radiative transfer equation.

(4) Mixed methods; usually in the form of a combination of broadband emission approximations and tabulation of transmittances.

2.1.1 Tabulation of transmission functions

A good example of this technique is the well known parameterization of CO_2 15 μm cooling rates proposed by Fels and Schwarzkopf (1981).

The transmission functions tabulated are computed with a line-by-line code, and then spectrally integrated. The expression for the cooling rate, q, is a semi-empirical relation between q and temperature in LTE:

$$q_i = q_i^\circ + \Sigma_j B_{ij}(T_j - T_j^\circ)$$

where the indexes denote atmospheric layers, Q° and T° are the cooling rate and kinetic temperature in a reference atmospheric state or profile, and B is a Curtis matrix that contains the atmospheric transmittances $\mathcal{T}_{ij}$. These authors showed that, since these transmittances are functions of the thermal structure between the layers i and j, just one single matrix is not appropriate.

They therefore proposed a number of reference temperature profiles, with precomputed transmittances, and examined the functional form of the dependence of the transmittances on the kinetic temperature in order to derive an interpolation method for any possible temperature structure. Their interpolation function, F_{ij}, depends on the layers' pressures and is proportional to the deviation from the reference temperature profile. They also found that a small number of reference T profiles was enough, and proposed to use only 3 profiles, 50 K apart from each other, T^-, T°, and T^+, and found the following simple interpolation

$$\mathcal{T}_{ij} = \mathcal{T}_{ij}^\circ + [\mathcal{T}_{ij}^- - \mathcal{T}_{ij}^+]\frac{F_{ij}}{50}$$

.

A drawback for non-LTE is that each hot band would require a special treatment, and the calculation of the source function does require an iteration process. However, many later studies employed some of the ideas outlined in this pioneering work.

2.1.2 Mixed methods

Fomichev et al. (1993) proposed a parameterization of the CO_2 15 μm cooling rate that has been employed in terrestrial GCM up to the lower thermosphere. Based on a previous parameterization of the transmittance derivative $d\mathcal{T}/dz$ by Akmaev and Shved (1982) for LTE conditions (below about 70 km, as this was the altitude of LTE departure thought at the time), a novelty of this study is the extension to the NLTE region. In particular, these authors considered two regions, a "radiative transfer" interval [70-85] km, where they employ a similar expression to Akmaev and Shved, and an "optically thin" interval [80-115] km, where they use a different expression. The idea behind this division is that in the [70-85] km region the departure from LTE is small because the atmosphere is still optically thick, and the exchange of radiation between layers is important. While the opposite tends to occur above around 85 km.

The expression they suggested for the cooling rate q_i at the layer i within the "radiative transfer" region is

$$q(x_i) = (1 - 3\phi_i)\ \Sigma_j\ [a_j(x_i) + b_j(x_i)\phi_i + c_j(x_i)\phi_i^2]\ \phi_j$$

where $\phi_j = exp(-960.24/T_j)$, T_j is the temperature at the layer j, and they make use of the dimensionless height $x = ln\ [1000/p(mb)]$. The coefficients $a_j(i)$, $b_j(i)$ and $c_j(i)$ prescribe the exchange of radiative energy between a given layer at x_i and all other layers x_j in the 626 fundamental (FB), 626 first hot (FH) and 626 second hot (SH) bands, respectively. This matrix of coefficients is precomputed and supplied by the authors. These values are chosen by numerical experimentation for a small set of 4 temperature profiles.

In the "optically thin" region, however, they employ a similar approach to that of Kutepov and Fomichev (1993), which is a recurrence formula, i.e., the cooling rate at a given altitude is obtained from that in the layer immediately below by

$$q(x_j) = C_1 \times [CO_2]\ [1 - \lambda_j] \times \tilde{q}(x_j)$$

where λ_j is a particular function of local parameters (temperature, rate coefficients, and number densities, all of them known) and the value of $\tilde{q}(x_j)$ is obtained using the recurrence formula

$$A_j \tilde{q}_j = A_{j-1} \tilde{q}_{j-1} - D_j \phi_j + D_{j-1} \phi_{j-1}$$

where A_j and D_j are simple linear relations of λ_j and some other coefficients d_j that are obtained from pre-computations of escape functions at each layer.

This recurrence formula is actually based on and derived from a 2-level model for the 626-FB. Kutepov and Fomichev (1993) recognized that this band is the largest contributor to the cooling rate in the upper mesosphere and lower thermosphere, and that this parameterization should be applied there. They mentioned that a similar scheme for other CO_2 bands is possible, and that the experimentation with a selected set of thermal profiles is particularly important in order to achieve a good merge between their "radiative transfer" and "optically thin" regimes.

While this scheme can not be exported directly to the Martian atmosphere, where V–V exchanges between different bands are very important, some of these ideas have been adapted, as we discuss below.

2.2 Approximate methods in Mars

Let us recall that in the Martian atmosphere a large number of bands of different strengths can give significant contributions to the cooling or heating of that atmosphere at altitudes where the optically thick transitions can not produce efficient coolings. Typical results were commented by López-Valverde et al. (1999). This situation is common to LTE calculations also.

The most computationally expensive aspect of a non-LTE model, particularly in the Mars atmosphere, is the computation of radiation transfer between atmospheric layers in those vibration-rotation bands which are very optically thick in the lowest altitudes of interest and very optically thin in the upper range. No simple approximations are really appropriate at all altitudes.

A frequent approach is the *cool-to-space*, which is usually very acceptable in the very high atmosphere, when the bands are optically thin. It eliminates contributions to and from other atmospheric layers and considers only the exchange term with the upper boundary. This has been extensively used in the past, specially when no other alternative was available.

This is the case of the parameterization developed by Bougher et al. (1986) for thermospheric GCMs for Venus and Mars. According to Bougher, the cooling rate is a function F of pressure, temperature and atomic oxygen. For the 626 fundamental band it is

$$F(p,t,[O]) = \frac{exp(-960/T)}{1+g(p,T,[O])}$$

where

$$g(p,t,[O]) = \frac{0.02}{pexp[40.6(\frac{1}{T_0^{1/3}} - \frac{1}{T^{1/3}})] \ \frac{[CO_2]+[O]}{[CO_2]+R[O]}}$$

$$R = \frac{5.25\times 10^{-14}\sqrt{T}}{5.20\times 10^{-15}\ [1+2\times 10^{-3}(T-220)]\ \frac{T}{273}}\ .$$

The cooling rate is then simply given by

$$q_{15\mu m}(T,p,[O]) = q_{15\mu m}(T_0,p,[O]_0)\ \times\ \frac{F(T,p,[O])}{F(T_0,p,[O]_0)}\ .$$

Bougher and coworkers computed cooling rates for the night and dayside hemispheres, as q_0 reference profiles, and then used this expression to interpolate between them (terminator, or any intermediate profile). However their expression is purely local and not very good below about 125 km for the 626-FB, which is the largest contribution to the total cooling rate at this height. This band becomes optically thin around this altitude or above (see below).

An even simpler expression was proposed by López-Puertas and López-Valverde (1995) at thermospheric altitudes,

$$q = 2E_{010}\,(k_{CO_2-O}[O] + k_{CO_2-CO_2}[CO_2]) \times [CO_2]exp(-E_{010}/kT) \qquad (1)$$

where E_{010} is the energy of the vibrational level 626(010), and also assumes optically thin conditions. This expression coincides with the approximation of Bougher and coworkers in the thermosphere, but again it is invalid below around 120 km.

Also the first attempt to include non-LTE within the present project (Read et al, 1998) considered optically thin conditions and is therefore of limited applicability in the upper mesosphere. They used $q_{NLTE}(T_K) = q_{LTE}(T_V)$ and the vibrational temperature, T_V, which is related to the source function of the transition, J, was computed from the approximate expression

$$J(T) = \frac{B(T)}{1+\frac{\epsilon'}{p+p_0}} \qquad (2)$$

where ϵ' is related to the ratio of collisional to radiative relaxation rates ϵ usually employed in non-LTE 2-level problems by extracting a linear pressure dependence in the collisional losses: $\epsilon' = (p+p_0)/\epsilon = (p+p_0)\times\frac{A}{l_{col}}$, being A and l_{col} the radiative and collisional specific loses, respectively. Here the parameters ϵ' and p_0 have complex dependencies on temperature and pressure, and were derived from fits to a small number of detailed calculations of 15 μm cooling rates performed with the Granada non-LTE model. This approach represents an improvement upon the López-Puertas and López-Valverde expression above, but is affected by the large sensitivity of the cooling rate to small errors in the source function (Fomichev et al. 1993). Also the expression for J is based on a 2-level system, which is very frequent in Earth's atmosphere simulations, but unable to reproduce V–V exchanges.

Another simple approximation to avoid non-LTE complications is to replace the thermosphere with an LTE buffer region at the top of the mesosphere. This may work for a benchmark case, but it is difficult to export generalities applicable to different cases, given the large dependence of the cooling rate on the local thermal structure and the usual thermospheric variation of the source function (see López-Valverde et al. 1998).

3 Development of the new parameterization

The basic strategy followed was mentioned above, namely: we started from the full non-LTE model (López-Valverde and López-Puertas, 1994a,b) and implemented successive simplifications to both the statistical equilibrium equations and to the expensive radiative transfer computation, until a very reduced system of levels and bands (with simple treatment of those two terms) remains.

A hierarchy of simplified non-LTE models has therefore been created. In order to validate them, the cooling rates were compared with the full non-LTE model. For this purpose, a number of reference scenarios are selected. They correspond to expected thermal regimes of the Martian atmosphere, for which very different values of the 15μm CO_2 cooling rate are obtained.

3.1 Reference model atmospheres

The driving idea behind the selection of the Martian atmospheric models is to guarantee a good approach in a diverse set of realistic conditions. The parameters of relevance for the cooling rates are: atmospheric temperature and pressure, number density, and the volume mixing ratios (vmr) of atomic oxygen and carbon dioxide (López-Valverde et al, 1999). An altitude range from 50 to 150 km was used. The top is needed in order to guarantee correct results below 130 km. Below 40 km the conditions in the lower atmosphere do not affect significantly the non-LTE behavior of the 15 μm bands since the LTE departure occurs much higher up.

After consideration of several atomic oxygen relative abundances from a diversity of sources, we have selected the profile by Nier et al. (1994) for average conditions and the COSPAR reference temperature structure. This vmr profile is employed for all reference atmospheres and conditions; the effect of the expected variability of atomic oxygen is discussed below.

Regarding the temperature structure of the mesosphere and lower thermosphere of Mars, we compared the Viking 1 and 2 entry profiles with two simulations of global mean radiative equilibrium temperatures for solar medium and solar maximum conditions (Bougher and Roble, 1991), with the Pathfinder entry data, and other model simulations. After considerations of the dispersion of absolute temperatures and their vertical gradients, we ended up with 8 selected profiles, as indicated in Table 1 and shown in Figure 1. The 8 reference temperature profiles also have their lower boundary at 50 km, as mentioned above, and use a similar sponge layer at the top height of 150 km.

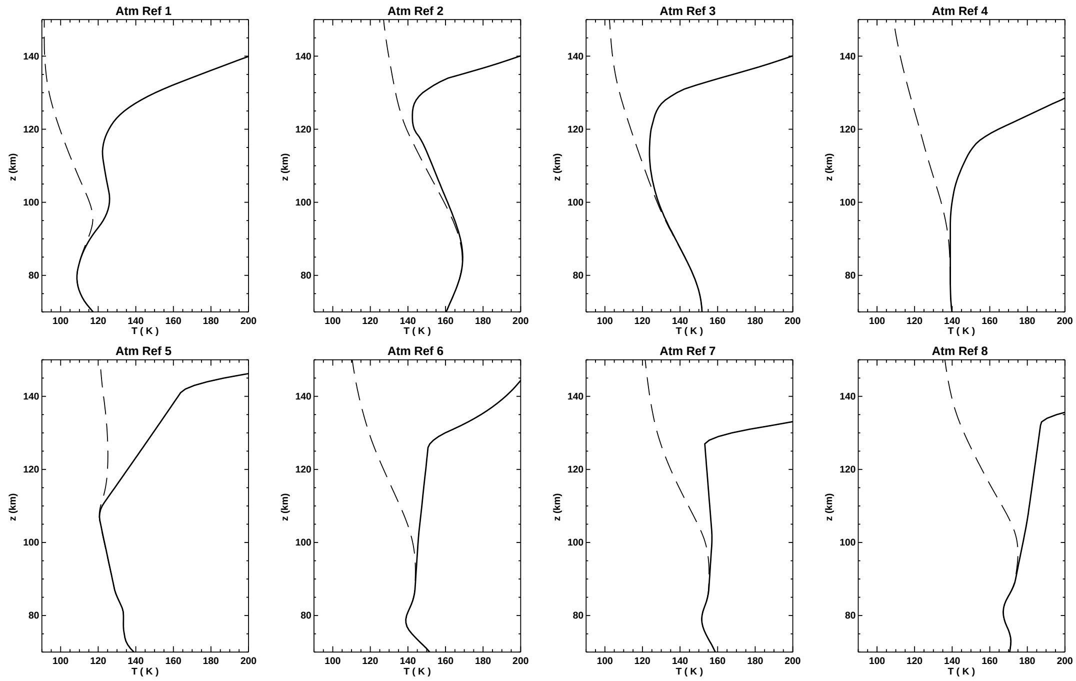

Figure 1: Set of eight reference temperature profiles of the Martian atmosphere. Solid line: T_K; dashed line: nighttime vibrational temperature of the 010-626 level.

Figure 1 also shows the vibrational temperature of the CO_2(010) state of the major isotope (626) to illustrate the variable departure from LTE (in terms of vibrational and kinetic temperature differences; see also López-Valverde et al, 1999). In order to better illustrate the thermal range covered by this set of profiles, all of them are plotted together in Figure 2.

Table 1. Reference model atmospheres

Atm.#	Conditions	Source (1)
1	Lat=20°N, L_s=142° LT=3am	Pathfinder ASI/MET (smoothed)
2	Mid Lat, Mid N Summer, 4 pm	1-D Rad.Eq. Simulation
3	Mid Lat, Mid N Summer, 3 am	1-D Rad.Eq. Simulation
4	Similar to ATM # 2	Viking 1 Entry (smoothed)
5	Lat=Equ., L_s=142°, LT=2pm	Oxford GCM
6	Lat=Equ., L_s=90°, LT=2pm	Oxford GCM
7	Lat=Equ., L_s=90°, LT=2am	Oxford GCM
8	Lat=Nort.Polar, L_s=90°, LT=2pm	Oxford GCM

(1) See Lopez-Valverde et al (2000) for more details.

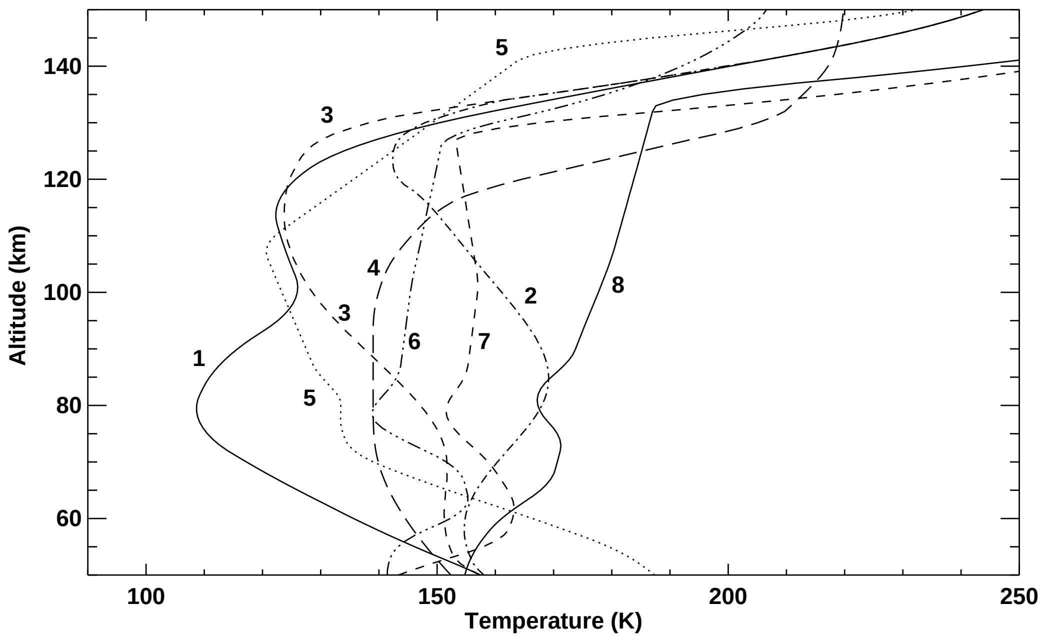

Figure 2: Set of eight reference temperature profiles of the Martian atmosphere selected for this work. Profiles are labelled as in Table 1.

3.2 Simplification of the statistical equilibrium equations

In general we can write the heating rate (or cooling rate if negative) as:

$$\begin{aligned} H(z) &= -\textstyle\sum_i Net\ Emission\ of\ Band_i \\ &= f(\ T_K(z), \nabla T_K(z), \rho(z), [O](z), [CO_2](z), k_{VT}, k_{VV}, ...) \end{aligned}$$

The complete non-LTE model used here as reference (López-Valverde and López-Puertas, 1994a,b) contains dozens of molecular vibrational levels and bands. The number of bands which actually contribute significantly to the thermal cooling at 15 μm is, however, much smaller. The CO_2 cooling rate is produced mainly by the 626 fundamental in the lower thermosphere (above 120 km approximately) and by the weaker isotopic bands (of the 636, 628 and 627 isotopes) and the 626 first hot bands in the upper mesosphere (largest contribution between 70 to 120 km approximately). The contribution profiles of the several CO_2 bands are shown in Figure 8 of the previous technical report by López-Valverde et al (1999), and discussed at length by López-Puertas and López-Valverde (1995). We summarize in Table 2 their non-LTE emission processes.

Table 2. Non-LTE mechanisms in the Martian atmosphere

CO_2 Band	Region	Emission Process (1)
626 FB	Lower thermosphere	$VT_1 + VV_2 + A_1$
ISO FB	Upper Mesosphere	$VT_1 + VV_{ISO} + A_{ISO}$
626 FH	Upper Mesosphere	$VT_1 + VV_2 + A_2$

(1) See Figure 2.

This is the key result that allows one to envisage a simplification of the system of bands and levels. Such simplified model, schematically shown in Figure 3, would necessarily require only 5 CO_2 levels and transitions. These are the FB of the 4 major CO_2 isotopes and the 626 first hot band (the 626 FH actually comprises 3 distinct vibrational-rotational transitions between the 3 Fermi resonant $CO_2(020)$ states and the (010) state; they are so close in energy that it is customary to group then together; Goody and Yung, 1989). We refer to this simplified model as "Simple#5".

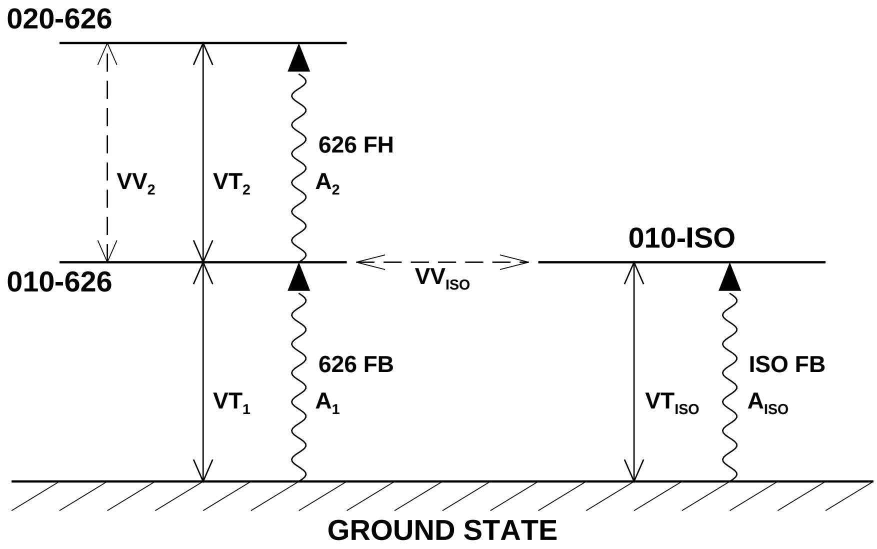

Figure 3: Schematic diagram of CO_2 levels and transitions in the simplified non-LTE model "Simple#5"

The cooling rates of a non-LTE model including only those levels and processes are shown in Figure 4, compared with the complete non-LTE model ("nominal" results) for all the reference atmospheres. In view of the large simplification in the number of levels and bands we appreciate that the agreement is very good for the eight cases, with maximum differences at the peak emission smaller than 20 % for reference atmosphere #8.

This is the simplest model that can be derived from a direct reduction in the number of transitions of the complete non-LTE model and still maintaining such excellent agreement with the nominal results. It includes radiative transfer in the 5 bands and exchanges of vibrational energy between the states by

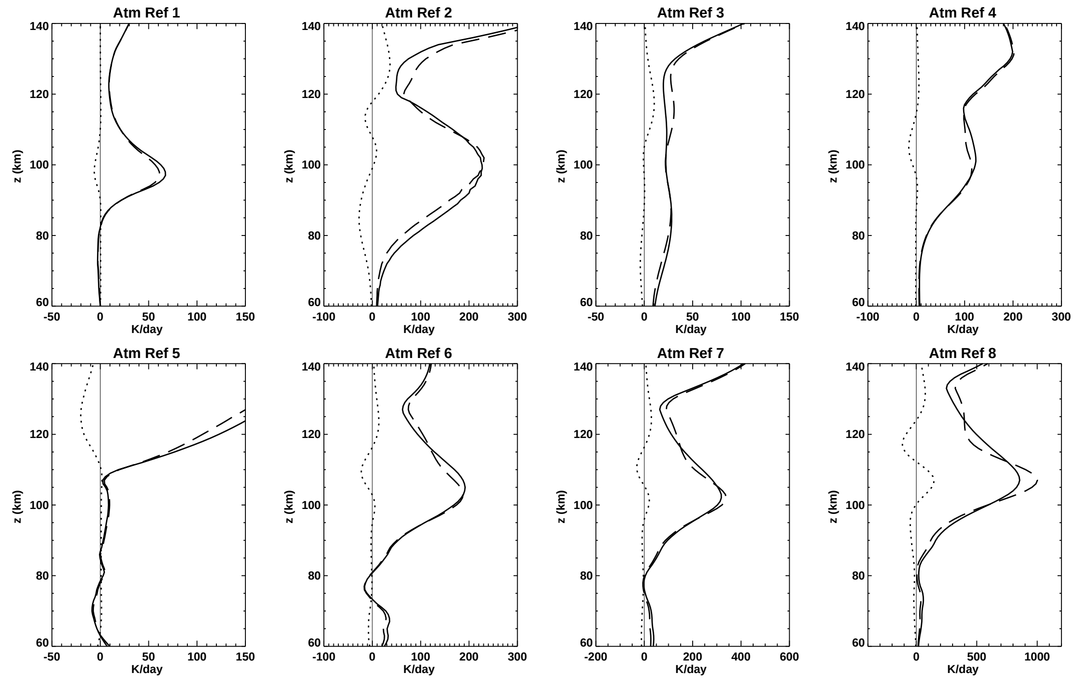

Figure 4: Cooling rates for the "Simple#5" version (dashed lines), compared to the nominal full non-LTE model (solid lines). Dots: difference simple–nominal. Note the different scales.

V–V and V–T collisions. This "Simple#5" version is still unacceptably expensive for a GCM. A further reduction is required, mainly in order to simplify the treatment of radiative transfer. An approximation to radiative transfer like the fast "cool-to-space" seems necessary, although it is surely not very appropriate for the strong 626 FB and for the weaker bands simultaneously. As a consequence, some additional adjustments to the processes of energy exchange between levels (collisions) are also foreseen at this stage in order to improve the agreement with the nominal results. Since those adjustments may be simpler the smaller the number of vibrational levels coupled, we continued the simplification process from this "Simple#5" model towards a version with a smaller number of levels and bands before applying any approximation to radiative transfer.

Such further simplification of the statistical equilibrium equations can be contemplated by noticing (see Table 2, for example) that the energy sources for all the weak bands (ISO FB and 626 FH) is the same: excitation of the (010)-626 state via V–T and subsequent V–V transfer to the isotopic-(010) or the 626-(020) states. Therefore, in a second simplification analysis we propose a non-LTE scheme with only two excited states and their respective radiative transitions, coupled to the ground states via V–T collisions, and including a V–V exchange between them. The first component would be the 626-(010) and the 626-FB while the second level could be an "equivalent state" comprising the other 4 states and their vibrational-rotational bands. We refer to this model as "Simple#2" and is shown in Figure 5.

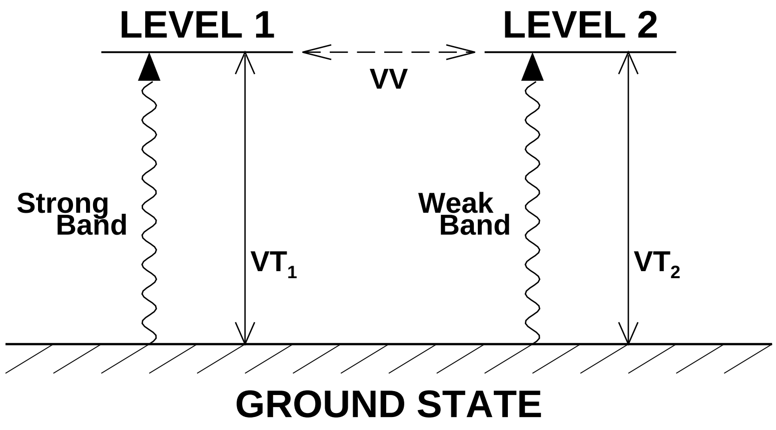

Figure 5: Further simplification of the Martian non-LTE model to only two excited vibrational states and transitions, called "Simple#2" in the text.

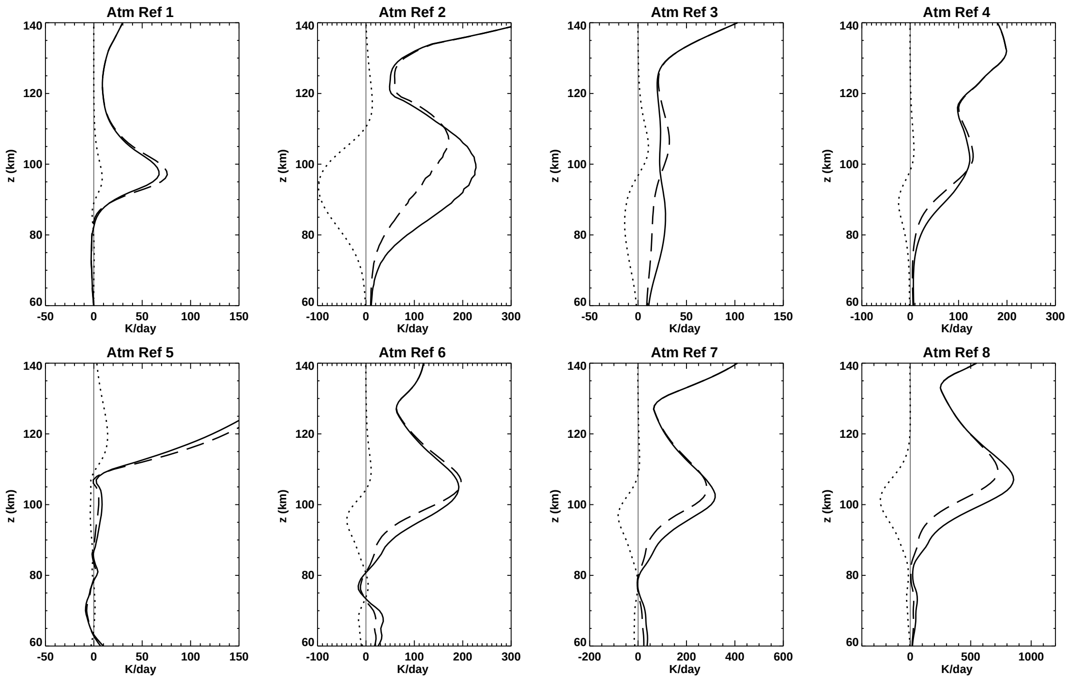

Figure 6: Cooling rates for the "Simple#2" version (dashed lines), compared to the nominal full non-LTE model (solid lines). Dots: difference simple–nominal.

The cooling rates obtained with this model, including full radiative transfer in the equivalent state are shown in Figure 6. The equivalent band contains all the lines of the 4 bands included (the FB of the three minor isotopes and the 626 FH). The exchange between layers in the full non-LTE model, as well as in the simplified versions, is treated with a line independent model that groups the spectral lines following an histogram in strengths (López-Valverde and López-Puertas, 1994a). Therefore, it is expected that the representative lines of the histogram boxes are now optically thicker than in the "Simple#5" version. This may be the reason for the systematic effect that the cooling rates in the mesosphere are slightly smaller now. Still the agreement with the nominal results is quite good in most atmospheres. Only in the cases of ref.atm.#2 and #3 the relative error in the peak emission has increased significantly, surely due to a specially large overestimation of the optical thickness in the strong lines of the 626 FH band.

3.3 Approximations to radiative transfer

The computation of radiation transfer between atmospheric layers makes this Simple#2 model very expensive computationally, and requires a simplification. The acceleration introduced here follows what could be classified like a mixed method in Section 2.1, it is a "cool to space" approximation with tabulated escape functions.

Under the cool-to-space approximation (CTS) the cooling rate of a given vibration-rotation band at a given altitude can be expressed as

$$q(z) = -\pi \; J(z) \; \frac{d\mathcal{T}(z,\infty)}{dz} \tag{3}$$

where $J(z)$ is the source function of the whole vibration-rotation band at the local height and $\mathcal{T}(z)$ the flux transmission to space at that altitude, integrated over the band. Evaluating the derivative analytically, using the definition of the strength of the band in terms of the Einstein coefficient, and the relation between the source function and the population of the upper level of the transition (neglecting stimulated emission), we can also express

$$q(z) = -hc\tilde{\nu} \; \frac{\beta}{4} A \; \mathcal{T}(z,\infty) \; n^*(z) \tag{4}$$

This simple expression of the radiative transfer equation allows to evaluate the cooling rate by a radiative transition at a given altitude if the population of the upper excited state, n^*, and the transmission to space in the band are known. The other terms it makes use of are the Einstein coefficient for spontaneous emission, a diffusivity factor for the angle integration (here we use $\beta = 1.8$), universal constants like h or c, and the central wavenumber of the band, $\tilde{\nu}$, all of which are well known.

Alternatively, using the following expression of the statistical equilibrium equation for the excited state

$$n^* \; \left[l_{col} + \frac{\beta}{4} A \mathcal{T}(z,\infty) \right] = P_{col} \tag{5}$$

we obtain

$$q(z) = -hc\tilde{\nu}\frac{\mathcal{T}/\epsilon}{(1+\mathcal{T}/\epsilon)}\ P_{col} \qquad \text{with} \qquad \epsilon = \frac{l_{col}}{\frac{\beta}{4}A} \simeq \frac{l_{col}}{A/2} \tag{6}$$

where l_{col} and P_{col} are the specific loses and the total productions of the excited state due to all collisional processes.

This cooling-to-space expression has two relevant improvements over previous optically thin studies: the allowance for V–V exchanges between excited states, and inclusion of the transmission to space or escape function $\mathcal{T}$. Particularly, when $\mathcal{T}$ is small the cooling rate will also be small, even if ϵ is small. This permits to apply the above expression to the optically thick bands in the mesosphere, a region not well modeled by the approximations of Bougher at al. (1986), López-Puertas and López-Valverde (1995) and Read et al (1998). In the optically thin conditions of the very upper atmosphere, the transmission to space can be approximated by $\mathcal{T} = 1$. Then, if ϵ is very small, it is obtained the eq.(1), suggested by López-Puertas and López-Valverde (1995). Also if V–T collisions dominate over non-thermal collisions, while $\mathcal{T} = 1$, eq.(6) reduces to eq.(2), that employed by Read et al (1998).

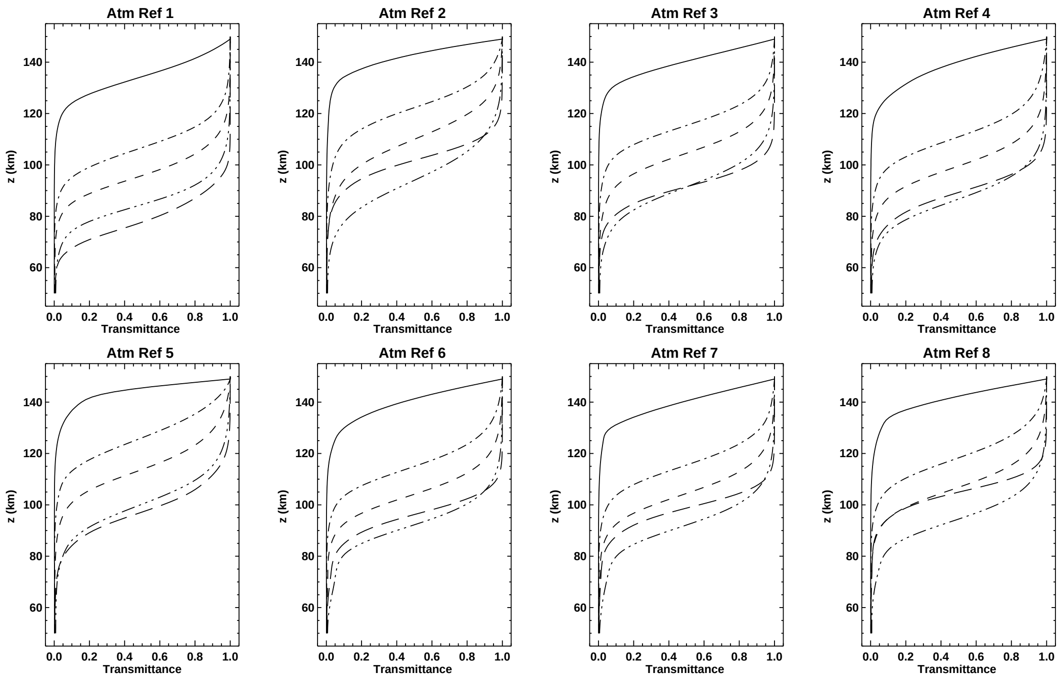

Figure 7: Escape functions for CO_2 bands. Solid: 626FB, dashed: 628 FB, dash-dot: 636 FB, dash-dot-dot-dot: 627 FB, long dash: 626 FH.

Figure 7 shows these escape functions for the 15 μm bands considered here and for all the ref. atmospheres. The strong 626 FB only reaches the optically thin regime ($\mathcal{T}$ close to unity) above 130 km in most cases (in the case of the dense ref.atm.#2 this only occurs well above 140 km). Figure 8 is the same plot but using log pressure as vertical coordinate. Improving that the vertical dispersion of the $\mathcal{T}$ profiles of the weak bands is small (by observing the

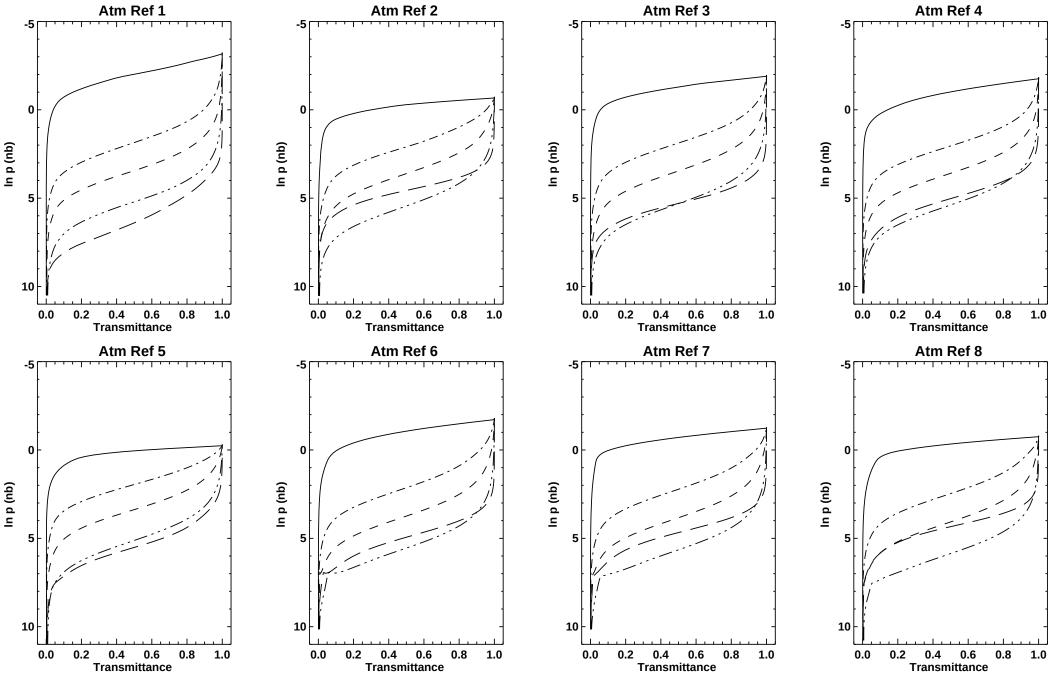

Figure 8: Same as Fig. 7 but as a function of pressure.

altitude where the transmission is 0.5), we have tabulated an average escape function profile for each band and for the "equivalent band" of the Simple#2 model, and this single profile is employed for any thermal structure, avoiding the need to compute the transmissions to space. Obviously this degrades the agreement with the nominal result, but only in a small amount.

The implementation of the CTS approximation in the weak band of the Simple#2 model, maintaining full radiative transfer in the strong band, results in the cooling rates shown in Figure 9. It is clear that the agreement with the nominal results is not good in several ref. atm., particularly in #2 and #3. The new cooling rates are larger than the nominal. The additional inclusion of CTS in the 626 FB also affects negatively, in the same direction: increasing the cooling rate. The results are shown in Figure 10. The increase is particularly notorious in ref.atm.#2, #5, #6 and #8. The effect in the lower mesosphere in atm.#5 is due to the overlapping between strong lines of the 626 FB, which is disregarded by the line independent model employed, but this is easily avoided by acting on the escape functions (this effect is eliminated in the final parameterization).

3.4 Other considerations for the parameterization

3.4.1 Collisional adjustment

In order to reduce the excess of cooling rate shown in Figure 10, a number of adjustments have been introduced.

A first overall improvement can be obtained by selecting different combinations of the weak bands' spectral properties when creating the "equivalent

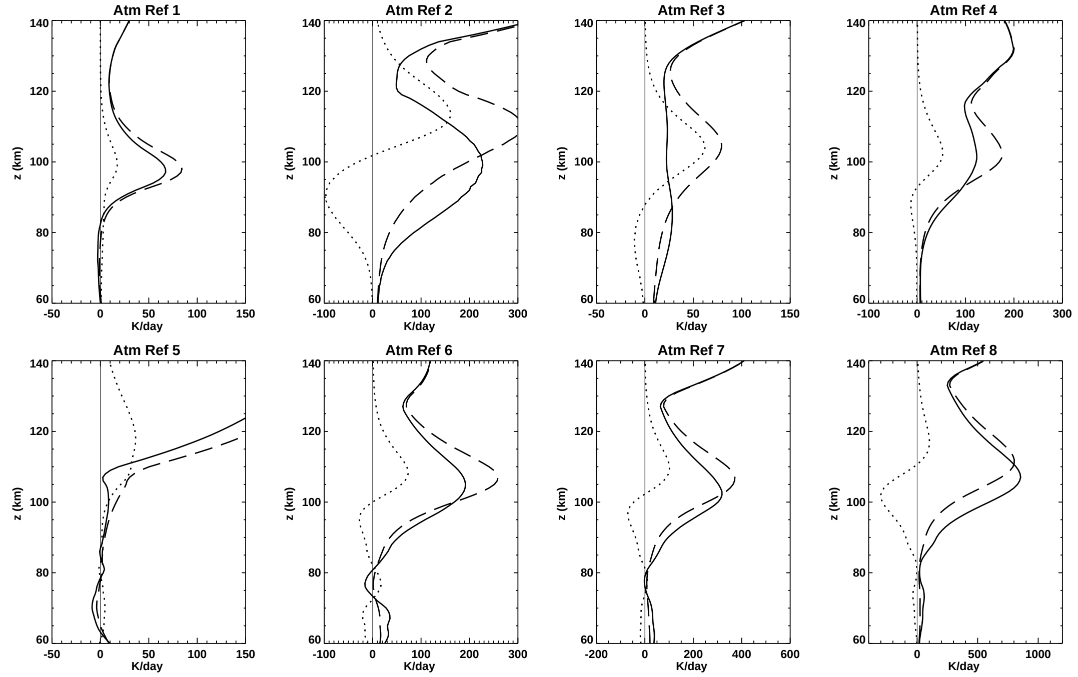

Figure 9: Cooling rates of the Simple#2 model when including cool-to-space in the weak band. Dashed: simple model; solid: nominal (full non-LTE); dots: simple–nominal

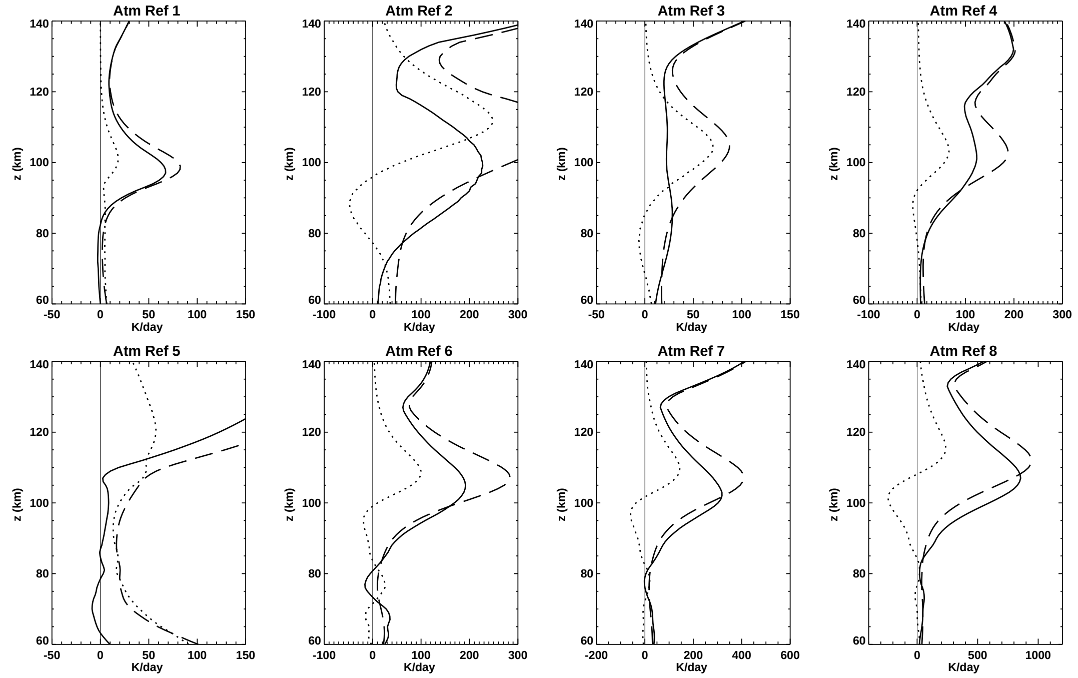

Figure 10: Same as Fig. 9 but with the addition of cool-to-space in the strong band. Dashed: simple model; solid: nominal (full non-LTE); dots: simple–nominal.

weak band" for the Simple#2 model; but this effect is actually small for any reasonable modification's magnitude (within current uncertainties).

After some experimentation, the best improvement by far can be achieved by acting on the collisional parameters. The rate coefficients for V–T and V–V exchanges were reduced by a factor 10, and the diffusivity factor was modified to $\beta = 1.66$. Also the overlapping error mentioned above was eliminated. The results are shown in Figure 11. These adjustments are not an ideal solution, since they surely depend on the set of reference atmospheres selected. At this stage of the study we opted for this in view of the significant improvement in comparison with the nominal results.

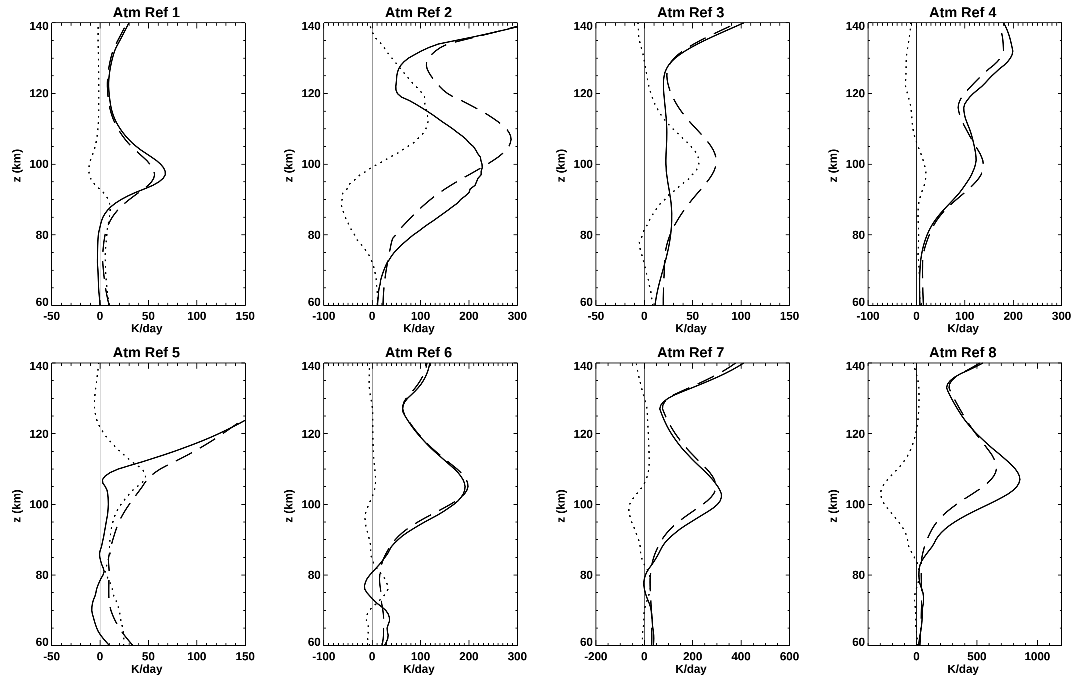

Figure 11: Cooling rates of the Simple#2 model with cool-to-space and collisional adjustment. Dashed: simple model; solid: nominal (full non-LTE); dots: simple–nominal

3.4.2 Volume mixing ratio effects

The atomic oxygen relative and carbon dioxide relative abundances are important parameters for the collisional excitation of the vibrational states, but they are variable. The atomic oxygen concentration decreases by several orders of magnitude from the Martian thermosphere where it is produced by photodissociation to the troposphere where only minor amounts after the vertical transport can be found. The variability in solar UV flux, photochemistry and turbulent motions affect atomic oxygen abundances at the peak cooling rate region. Also the concentration of the major atmospheric constituent in Mars, which is well mixed throughout the troposphere and mesosphere, declines with height above the homopause, around 125 km, due to molecular diffusion. In addition to these changes there are variations in total number density of the neutral atmosphere, as illustrated by the annual surface pressure cycle. These variations can indirectly incorporated into the parameterization outlined here by a proper selection of the reference model atmospheres, and by the use of pressure as vertical coordinate. Changes in total density do not affect the [O] to [CO_2] ratio, nor consequently, the population of the excited states of the bending mode of vibration.

The ideal solution would be to calculate the mixing ratios of these species at each altitude and solar illumination on line within the GCM. At present this is not done and a single profile of abundances has been selected for the current parameterization. The values of atomic oxygen, carbon dioxide and the other two major collisional partners, NO and CO, have been taken from the model of Nier et al. (1994), as a function of altitude, and are shown in Figure 12.

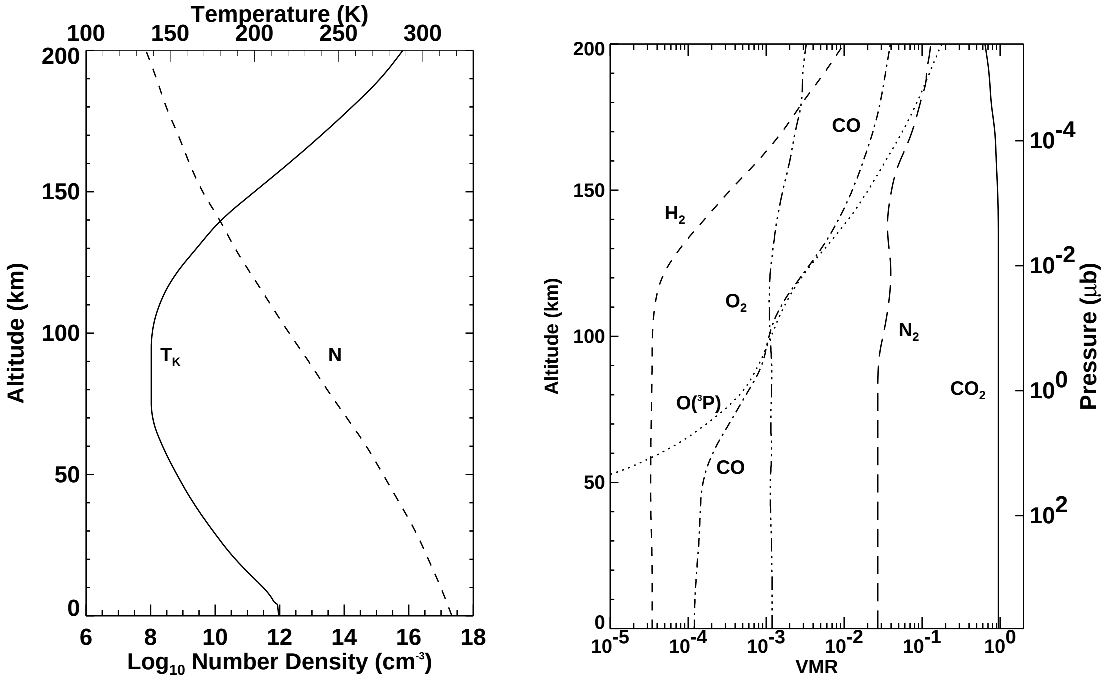

Figure 12: Model atmosphere based on the photochemical 1-D model of Nier et al., Icarus, 1994. Left: temperature and density; right: vmr of the different species, as indicated.

In order to interpolate these values to a particular atmospheric profile, a consideration about the vertical coordinate to use is necessary. First, the vertical variation of atomic oxygen and CO_2 depend on local density, optical depth of solar radiation, and other pressure dependent variables; we should therefore use pressure as the coordinate for that interpolation. Second, the tabulation of the chosen mixing ratios is to be given as a single profile of pressure; so we need to transform the mixing ratios to a pressure coordinate. In order to do this, we took the reference pressure used in the photochemical model of Nier et al. and built the vmr table for our parameterization.

The approximation of using a single atomic oxygen profile would be eliminated in the future if a chemical code computes the atomic oxygen profile on line. Meanwhile, we will have an uncertainty at thermospheric altitudes from the natural variability of atomic oxygen there. Actually all these changes are most important above 120 km. Below 120 km the changes introduced are much smaller. So this constant VMR profile for all conditions should be reasonably good for the altitude range of interest at present.

3.4.3 Merging with the LTE region

Among the particular characteristics and approximations of the reference non-LTE model, we have already mentioned that radiative transfer is described with a line-independent-model which treats overlapping among lines in a crude way; therefore, our cooling rate may differ from other models' in the LTE region. Hence, some care must be taken in order to ensure that the proposed parameterization can be implemented in any GCM, whichever radiative transfer scheme is used in the LTE region. A simple solution is to merge the non-LTE results obtained here to the LTE results of the external model (the code where the parameterization is to be implemented).

A smooth switch, as a function of altitude, $\sigma(z)$, is proposed for this purpose so that at each altitude we can obtain the cooling/heating rate as a combination of the external LTE code's result ($q^{LTE}(z)$) and the supplied NLTE parameterization, ($q^{NLTE}(z)$):

$$q = q^{NLTE}\ \sigma + q^{LTE}\ (1-\sigma) \tag{7}$$

We propose here the following expression:

$$\sigma(z) = 0.5\ \left[\ 1 + tgh(\frac{z - z_s}{z_w})\ \right] \tag{8}$$

where the vertical coordinate to use is $z = -ln\ p(nb)$, and the free parameters z_s and z_w define the altitude of the transition region and its width, respectively. From our LTE and non-LTE runs, the following choice of values seems very adequate for all the ref. atmospheres in this study: ($z_s = -5.5$, $z_w = 0.5$). This value of z_s correspond to altitudes between 82 km in ref.atm. #1 and 97 km in ref.atms. #5 and #8.

3.4.4 Non-LTE modeling uncertainties

It is important to realize that there is a number of uncertainties in the reference non-LTE calculations due to a number of reasons. It is therefore convenient to evaluate the potential impact they may have on the parameterization proposed.

The non-LTE theoretical model predictions are subject to uncertainties due to approximations in both the solution of the radiative transfer and the set up of the different levels' statistical equilibrium equations. In addition, it requires a number of input parameters, like spectroscopic data or isotopic abundances, and most importantly, rate coefficients that describe the energy transfer during collisions, all of which are known with a limited precision only.

Detailed analysis of the dependence of the model results on those input data and how current uncertainties in them affect the vibrational populations and the IR balance by CO_2 have been carried out previously by López-Valverde and López-Puertas (1994a,b) and López-Puertas and López-Valverde (1995), respectively. We base our analysis on their results, considering here only the parameters with largest effects.

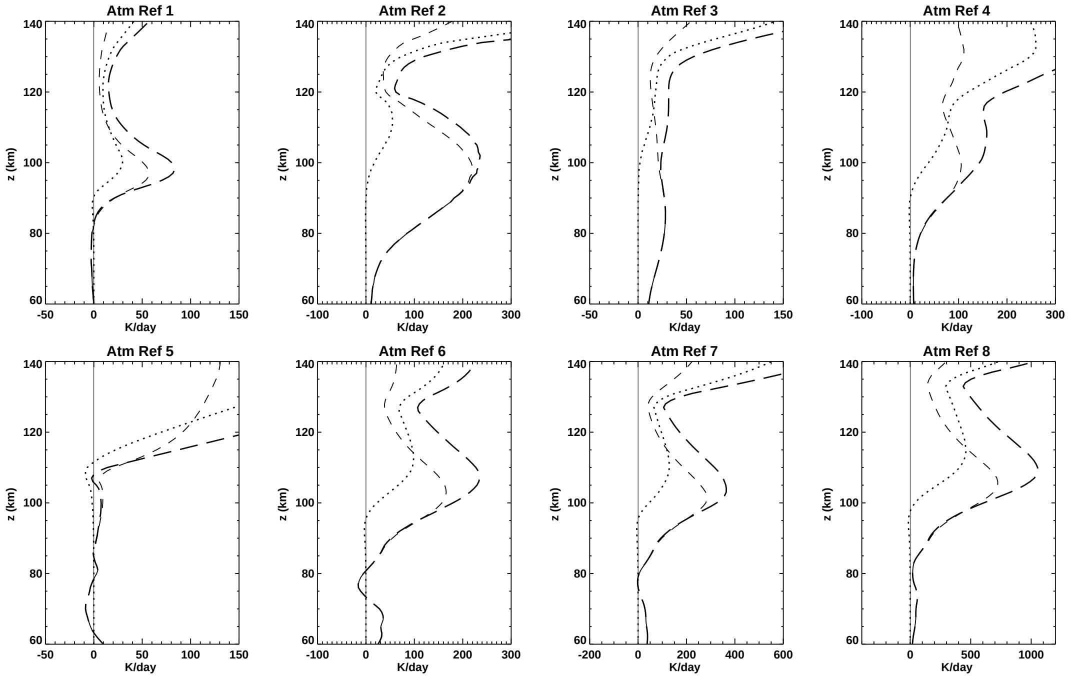

Figure 13: Effect of increasing and reducing the rate coefficient of V–T collisions between CO_2 and atomic oxygen by a factor 2. Long dash: increased rate; short dash: decreased rate; dots: increased – reduced.

The rate coefficient for V–T collisions of CO_2 with atomic oxygen and the relative abundance of atomic oxygen in the upper atmosphere are with no doubt the most serious uncertainties in 15 μm cooling rate calculations. Both enter the collisional losses in the same term, and therefore produce the same effect. An uncertainty of a factor 2 is still present in the rate coefficient. Regarding the variability of atomic oxygen, this is smaller than higher up in the thermosphere, and a factor 2 again may embrace potential changes below 120 km. The neglect of these changes in the parameterization would produce the same effect as that obtained by López-Puertas and López-Valverde (1995) in their sensitivity study for such change, but this depends very much on the thermal structure used. We have performed calculations with the full non-LTE model for the eight reference atmospheres employed in the parameterization after introducing a large change of a factor 4 in the rate coefficient (increased and reduced by 2). This is equivalent to a similar change in the atomic oxygen profile at all altitudes, which is surely an overestimation of its variability. The comparison with the nominal results is shown in Figure 13. The relative importance of the atomic oxygen uncertainty increases with altitude and above 130 km is more than 50% in most profiles. Examination of these results and the accuracy of the parameterization shown in Figure 11 reveals that the uncertainty in atomic oxygen is comparable or larger than the error in the parameterization at 100 km for ref. atmospheres #1, #4, #6 and #7, around 115 km for ref. atmospheres #3, #5, and #8, and above about 130 km for ref. atm. #2.

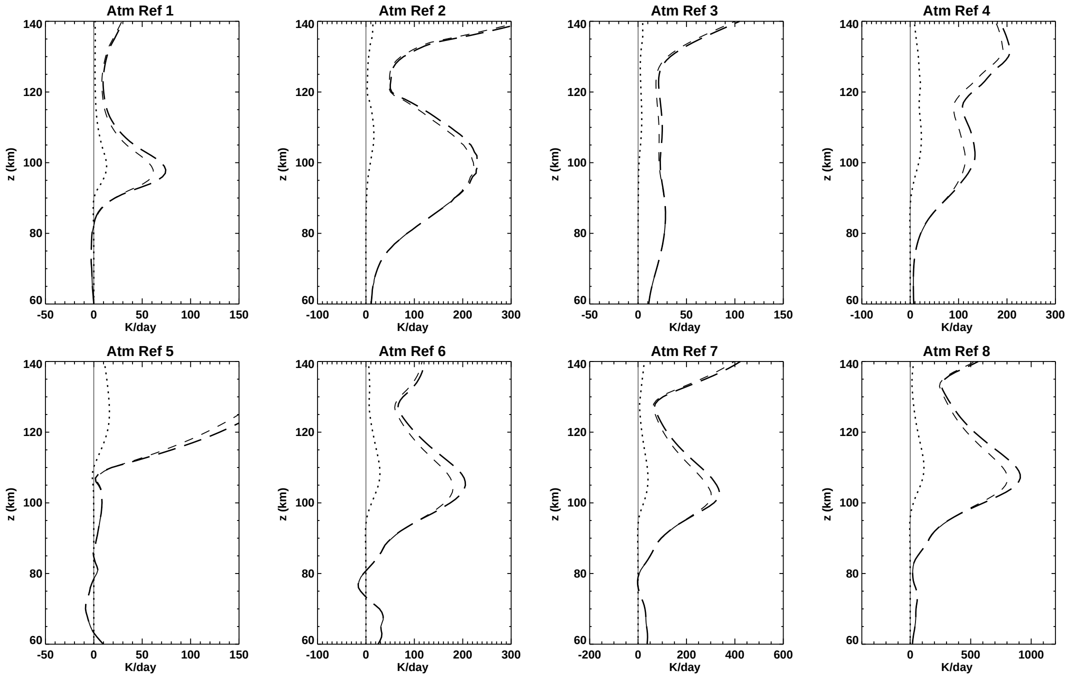

Figure 14: Effect of increasing and reducing the rate coefficient of V–T collisions between CO_2 and CO_2, N_2 and CO by a factor 1.4. Long dash: increased rate; short dash: decreased rate; dots: increased – reduced.

Another important rate coefficient in the non-LTE model with a significant uncertainty, according to the discrepancy between laboratory experiments, is the V–V exchange between the CO_2 (010)-626 state and the same level of the minor isotopes and the $(0,\nu_2,0)$ overtones. The effect obtained by López-Puertas and López-Valverde (1995) in the cooling rate was very small for the COSPAR temperature profile they used, and we have confirmed the same for all the reference atmospheres in this study.

The only other single rate coefficient with non-negligible effects is the V-T relaxation with the rest of the atmospheric molecules, mainly CO_2. An uncertainty factor 2 has been used (increased by 1.4 and reduced by the same factor). The results are shown in Figure 14 for the eight reference atmospheres. The effect is larger at the peak of the cooling rate, and amounts to less than 20 % in all cases. This is similar to the parameterizaion error in atmospheres #1, #4, #6 and #7 above about 100 km; but in all the other cases this rate coefficient has a much smaller impact.

The radiative transfer code used in our non-LTE reference model is specially designed for the upper atmosphere. It includes a number of approximations to radiative transfer in the nominal code for computing atmospheric transmittances, like the Curtis-Godson for large atmospheric paths, an approximate treatment of overlapping between lines using the Goody random model, and averaging of spectral line intensities and widths in the histogram technique. Comparisons with a general purpose line-by-line code have been performed in the past (López-Valverde et al., 1998) to evaluate the quality of these assumptions in the Mars atmosphere. The agreement in the region of interest (50-120 km) is less than 5 %, which is smaller than the current parameterization discrepancy with the nominal calculation. Although small, a future computation of transmission functions with a line-by-line code could easily eliminate effect.

4 Tabulation and implementation

The cooling rate is computed according to the scheme labelled Simple#2, which includes 2 excited states with V–T collisions with the ground state and coupled between them by V–V exchanges. They emit according to a cool-to-space form with escape functions in the two bands, one stronger than the other, representing the 626 FB and the weaker isotopic FB and 626 FH bands. The cooling is simply computed by

$$\begin{aligned} q_{15\mu m}(z) &= q_{strong}(z) + q_{weak}(z) \\ &= -hc\frac{\beta}{4}\ [\ \tilde{\nu}_1 A_1 \mathcal{T}_1(z,\infty)\ n_1^*(z)\ +\ \tilde{\nu}_2 A_2 \mathcal{T}_2(z,\infty)\ n_2^*(z)\ ] \end{aligned} \tag{9}$$

where the populations of the excited states n_1^* and n_2^* are obtained by solving analytically the linear system of couple equations formed by the two statistical equilibrium equations in Simple#2 (see Section 3.2). Therefore, in addition to rate coefficients, Einstein emission coefficients, radiation constants, isotopic abundances and other constants, the calculation of $q_{15\mu m}(z)$ within this parameterization just requires to know the local values of temperature and pressure, and to read the vmr of CO_2 and its major collisional partners (atomic oxygen, CO and N_2), and the escape functions of the strong band (the 626-FB, lets say band #1) and of the equivalent weak band (band #2) from the tabulation (see below).

4.1 Computational scheme

The steps to follow in order to compute the cooling rate are (see the delivered subroutine for more details):

STEP 1: Set up of needed constants

These are the Einstein spontaneous emission coef. for the strong and weak bands (A_1 and A_2), the central wavenumber of the two bands, the isotopic abundances of the two bands, the velocity of light and the Planck constant.

STEP 2: Get the local temperature and pressure

This parameterization, used as a subroutine, must be supplied with the temperature and pressure at each grid point.

STEP 3: Read the tabulation

The values read in are the vmr of CO_2, $O(^3P)$, N_2 + CO, and the escape functions for the two bands ($\mathcal{T}_1$ and $\mathcal{T}_2$). These values are then interpolated to the local pressure supplied in *STEP 2*

STEP 4.a: Compute rate coefficients

These are four different rate coefficients and their inverse rates, all of them functions of the local temperature obtained in *STEP 2*. They are the V–T collsions with atomic oxygen, the V–T collisions with CO_2, the V–T collisions with N_2 and CO (the same for these two compounds), the the V–V exchanges between (010) states of the two isotopic species.

STEP 4.b: Compute ground state populations

The ground state populations n_1 and n_2 of the two isotopes are the lower states of the two bands, and are obtained from the isotopic abundances (*STEP 1*), the CO_2 vmr (*STEP 3*), and the local temperature and pressure (*STEP 2*).

STEP 5: Compute collisional productions and loses

There are six different terms that are needed here:

- collisional production of state 1 from all V–T processes in which it participates, P_1
- specific collisional loses of state 1 du to all V–T and V–V processes in which it participates, l_1
- collisional production of state 2 from all V–T processes in which it participates, P_2
- specific collisional loses of state 2 from all V–T and V–V processes in which it participates, l_2
- specific collisional production of state 1 via V–V exchange from the (010) state of the other isotope, p_{12}
- specific collisional production of state 2 via V–V exchange from the (010) state of the other isotope, p_{21}

STEP 6: Compute the population of the excited states

The populations n_1^* and n_2^* that appear in eq.(9) can be obtained from the production and loss terms of *STEP 5*, the ground state populations from *STEP 4.b*, and some constants from *STEP 1*. First n_2^* must be obtained using

$$n_2^* = \frac{l_1\ P_2\ +\ \alpha_2\ P_1\ p_{21}}{l_1\ l_2\ -\ p_{12}\ p_{21}}$$

and then n_1^* can be computed using

$$n_1^* = \frac{P_1}{l_1}\ +\ \alpha_1\ \frac{n_2\ p_{12}}{l_1}\ n_2^*$$

where α_1 and α_2 are combinations of molecular and universal constants from *STEP 1*.

STEP 7: Compute the cooling rate

This is obtained with eq.(9), where all the terms have already been obtained in previous steps.

4.2 Tabulation

The tabulation of these parameters, as a function of pressure, that has been delivered is presented in Table 3.

Table 3 (Part I). Tabulation of delivered parameters.

lnp(nb)	Esc.F.#1	Esc.F.#2	CO2 vmr	O3P vmr	N2+CO vmr
12.0000	0.000458112	0.00198992	0.950000	5.06756e-08	0.0271412
11.0000	0.000458112	0.00198992	0.950000	9.16539e-07	0.0271464
10.8000	0.000458112	0.00198992	0.950000	1.68217e-06	0.0271490
10.6000	0.000458112	0.00198992	0.950000	3.00843e-06	0.0271523
10.4000	0.000458112	0.00198992	0.950000	5.03151e-06	0.0271558
10.2000	0.000458112	0.00198992	0.950000	8.07489e-06	0.0271617
10.0000	0.000458112	0.00198992	0.950000	1.23137e-05	0.0271672
9.80000	0.000458112	0.00198992	0.950000	1.79029e-05	0.0271749
9.60000	0.000458112	0.00198992	0.950000	2.45308e-05	0.0271837
9.40000	0.000458112	0.00198992	0.950000	3.27431e-05	0.0271943
9.20000	0.000458112	0.00198992	0.950000	4.26692e-05	0.0272058
9.00000	0.000458112	0.00201376	0.950000	5.44396e-05	0.0272189
8.80000	0.000458112	0.00209450	0.950000	6.78865e-05	0.0272326
8.60000	0.000458112	0.00222993	0.950000	8.33147e-05	0.0272483
8.40000	0.000458112	0.00242056	0.950000	0.000100148	0.0272661
8.20000	0.000458112	0.00268018	0.950000	0.000118846	0.0272848
8.00000	0.000458112	0.00304398	0.950000	0.000139681	0.0273054
7.80000	0.000458112	0.00343896	0.950000	0.000164909	0.0273279
7.60000	0.000458112	0.00380282	0.950000	0.000193617	0.0273514
7.40000	0.000458112	0.00420622	0.950000	0.000225161	0.0273775
7.20000	0.000458112	0.00476121	0.950000	0.000260834	0.0274048
7.00000	0.000458112	0.00801698	0.950000	0.000301501	0.0274345
6.80000	0.000461707	0.0119947	0.950000	0.000344953	0.0274672
6.60000	0.000476886	0.0169149	0.950000	0.000391011	0.0275021
6.40000	0.000495638	0.0224497	0.950000	0.000440377	0.0275404
6.20000	0.000520935	0.0285244	0.950000	0.000490820	0.0275826
6.00000	0.000555511	0.0354813	0.950000	0.000543200	0.0276340
5.80000	0.000601219	0.0439264	0.950000	0.000595335	0.0277013
5.60000	0.000663734	0.0546248	0.950000	0.000645420	0.0278220
5.40000	0.000750691	0.0675367	0.950000	0.000693166	0.0279707
5.20000	0.000863474	0.0829931	0.950000	0.000743729	0.0281759
5.00000	0.00100900	0.101717	0.950000	0.000793710	0.0284339
4.80000	0.00119642	0.123422	0.950000	0.000844394	0.0287587
4.60000	0.00142690	0.148468	0.950000	0.000894318	0.0291600

Table 3. (Part II). Tabulation of delivered parameters.

lnp(nb)	Esc.F.#1	Esc.F.#2	CO2 vmr	O3P vmr	N2+CO vmr
4.40000	0.00171398	0.177096	0.950000	0.000944732	0.0296561
4.20000	0.00206663	0.208816	0.950000	0.000994964	0.0302558
4.00000	0.00248974	0.244003	0.950000	0.00104901	0.0309922
3.80000	0.00301578	0.282013	0.950000	0.00110008	0.0318062
3.60000	0.00364350	0.322559	0.950000	0.00116302	0.0327010
3.40000	0.00440323	0.365542	0.950000	0.00122989	0.0335635
3.20000	0.00532066	0.410518	0.950000	0.00130026	0.0344388
3.00000	0.00640456	0.457384	0.950000	0.00137131	0.0353327
2.80000	0.00772069	0.505358	0.950000	0.00145556	0.0362143
2.60000	0.00925684	0.553627	0.950000	0.00155186	0.0370941
2.40000	0.0110905	0.600472	0.950000	0.00166328	0.0379315
2.20000	0.0132374	0.644807	0.950000	0.00177802	0.0387626
2.00000	0.0157643	0.687185	0.950000	0.00191546	0.0395524
1.80000	0.0187388	0.727429	0.950000	0.00207503	0.0403071
1.60000	0.0222072	0.764734	0.950000	0.00224903	0.0410071
1.40000	0.0263099	0.798562	0.950000	0.00247117	0.0416229
1.20000	0.0310614	0.828699	0.950000	0.00271728	0.0421231
1.00000	0.0366948	0.854797	0.950000	0.00299739	0.0425167
0.800000	0.0432373	0.877717	0.950000	0.00333582	0.0427964
0.599999	0.0515022	0.897874	0.950000	0.00373507	0.0429773
0.400000	0.0621455	0.915258	0.950000	0.00420819	0.0430488
0.200000	0.0777212	0.929904	0.950000	0.00476887	0.0429638
0.00000	0.0992027	0.942381	0.950000	0.00542558	0.0428049
-0.200000	0.131155	0.952906	0.950000	0.00620815	0.0426788
-0.400001	0.179470	0.962173	0.950000	0.00714473	0.0426822
-0.600000	0.258913	0.970191	0.950000	0.00828545	0.0429426
-0.800000	0.380549	0.976437	0.949619	0.00951779	0.0434634
-1.00000	0.530450	0.981501	0.947694	0.0108140	0.0442559
-1.20000	0.643180	0.985406	0.945830	0.0122359	0.0453038
-1.40000	0.741061	0.988560	0.944016	0.0136870	0.0465879
-1.60000	0.826336	0.991111	0.940557	0.0151495	0.0480262
-1.80000	0.922787	0.993653	0.937068	0.0167196	0.0496303
-2.00000	0.997203	0.995561	0.932366	0.0185485	0.0514885
-3.00000	1.00000	1.00000	0.893661	0.0336252	0.0691651

5 Summary and Future improvements

A parameterization of the CO_2 infrared cooling rates has been developed and is working operationally in the Martian GCM. It is a 3-level system (2 excited states coupled with V–V exchanges) with a cool-to-space approximation that employs tabulated escape functions as function of pressure. This is based on simplified versions of a complete non-LTE model, which is taken as a benchmark for comparisons, after extensive analysis for a pre-defined set of 8 reference atmospheres. This improves upon any existing study of approximations for the upper atmosphere of Mars since it qualitatively and quantitatively compares well with the major features of the 15 μm cooling in the upper mesosphere and lower thermosphere, reproducing the non-LTE mechanisms involved, like collisional to radiative control of the excitation process and V–V exchange from the 626-(010) state to the isotopic-(010) and to the 626-(020) states.

The cooling rates parameterized here represent good approximations to the nominal values of the full non-LTE model for several reference atmospheres, but the agreement is not very good in warm and dense mesospheres (ref.atm.#2 and #8). We have found that the reduction of the number of statistical equilibrium equations between the key emission energy levels is not the major reason for the disagreement, but rather the approximation to radiative transfer in the "equivalent weak band" of the simplified model, and in the stronger 626 fundamental. We also found that simple adjustments to collisional processes (applied to all the reference model atmospheres) are able to produce (re-establish) good agreement in most atmospheres, although this is somehow an "ad hoc" method which could be very dependent on the particular selection of reference atmospheres, and should be eventually replaced by a more rigorous approach.

Therefore we foresee the parameterization should be improved in the future with some study oriented toward the replacement of the collisional adjustments. In particular, a number of recommendations follow, listed in order of their expected improvement:

(1) The usage of an approximation to radiative transfer which does not only includes emission to space but also exchange with the closer adjacent layers may be very beneficial. Recent work in this direction has been carried out within the present project by the LMD group (Hourdin et al, 1999) and offers an interesting possibility for an improved parameterization in a future.

(2) Depending on computer resources, still a simpler alternative to (1) can represent improvements to the present cool-to-space scheme. For example, using a tabulation of line-by-line computed escape functions for the isotopic fundamental transitions combined with an on-line computation of the escape functions of the 626 fundamental and first hot bands; i.e., these two transitions would not be tabulated. This would improve the cooling rates in atmospheric situations with extreme pressure and temperature structures.

3) An on-line computation of atomic oxygen abundances, even with a simplified photochemistry, should be able to impose realistic variations at different time scales. This would eliminate another tabulated input to the parameterization and would reduce the current uncertainty due to those variations.

(4) A reduction of the statistical equilibrium equations to just 2 excited states and 2 fundamental transitions may be an oversimplification. The usage of 5 excited states that include the 626 FH band and the 4 major isotopes' fundamentals, or at least 3 excited states (with explicit inclusion of the 626 FH, differentiated from the ISO FB), should produce a better agreement in a larger number of atmospheres.

(5) A different and larger set of model atmospheres, from TES data for example, and with a noisy/wavy nature, should also be employed to validate

the parameterization scheme.

Finally, let us recall that the simplification process from a full non-LTE model to the present fast scheme has resulted in a very interesting hierarchy of simple non-LTE models. This will be very useful for future improvements to the parameterization, since it will be possible to investigate improvements of different aspects, like radiative transfer, and then “walk up” steps along this hierarchy of models, until the compromise computational cost / precision established in the GCM is met.

6 References

Akmaev R. A. and Shved G. M., Parameterization of the radiative flux divergence in the 15-μm CO_2 band in the 30-75 km layer, *J. Atmos. Terr. Phys., 44*, 993-1004, 1982.

Bougher, S.W., R. E. Dickinson, E. C. Ridley, R. G. Roble, A. F. Nagy, and T. E. Cravens, Venus Mesosphere and Thermosphere II. Global Circulation, Temperature and density variations *Icarus, 68*, 284-312, 1986.

Bougher, S. W., and R. G. Roble, Comparative terrestrial planet thermospheres, 1, Solar cycle variation of global mean temperatures, *J. Geophys. Res., 96*, 11045-11055, 1991.

Fels S. B. and M. D. Schwarzkopf, An efficient, accurate algorithm for calculating $CO_2$2 15 μm band cooling rates, *J. Geophys. Res. 86*, 1205-1232, 1981.

Fomichev, V. I., A. A. Kutepov, R. A. Akmaev, and G. M. Shved, Parameterization of the 15 μm CO_2 band cooling in the middle atmosphere (15-115 km), *J. Atmos. Terr. Phys., 55*, 7-18, 1993.

Goody, R. M., and Y. L. Yung, *Atmospheric Radiation: Theoretical Basis. 2nd Ed.*, Oxford University Press, New York, 1989.

Hourdin, C., J-L Dufresnes, R. Fournier and F. Hourdin New model radiation schemes, parameterization and validation. *ESA Technical Report, WP6.1 CCN2 extension of ESA 11369/95/NL/JG*, Nov 9, 1999.

Kutepov, A. A. and V. I. Fomichev, Application of the second order escape probability approximation to the solution of the NLTE vibration-rotational band radiative transfer problem, *J. Atmos. Terr. Phys., 55*, 1-7, 1993.

López-Puertas, M. and M.A. López-Valverde, Radiative energy balance of CO_2 non-LTE infrared emissions in the Martian atmosphere. *Icarus, 114*, 113-129, 1995.

López-Valverde, M. A. and M. López-Puertas 1994a. A non-local thermodynamical equilibrium radiative transfer model for infrared emissions in the atmosphere of Mars. 1. Theoretical basis and nighttime populations of vibrational states. *J. Geophys. Res., 99*, 13093-13115, 1994a.

López-Valverde, M. A. and M. López-Puertas 1994b. A non-local thermodynamical equilibrium radiative transfer model for infrared emissions in the atmosphere of Mars. 2. Daytime populations of vibrational levels, *J. Geophys. Res., 99*, 13117-13132, 1994b.

López-Valverde, M. A., D. P. Edwards, M. López-Puertas and C. Roldán, Non-local thermodynamic equilibrium in general circulation models of the Martian atmosphere 1. Effects of the local thermodynamic equilibrium approximation on thermal cooling and solar heating *J. Geophys. Res., 103*, 16799-16811, 1998.

López-Valverde, M. A., M. López-Puertas and C. Roldán Non-LTE effects in the atmosphere of Mars *ESA Technical Report, WP6.3 CCN2 extension of ESA 11369/95/NL/JG*, November 18, 1999.

López-Valverde, M. A., R. M. Haberle and M. López-Puertas Non-LTE radiative mesospheric study for Mars Pathfinder entry *Icarus, 146*, 360-365, 2000.

Nier et al., A photochemical model of the Martian Atmosphere, *Icarus, 111*, 124-150, 1994.

Read, P. L., F. W. Taylor, S. R. Lewis and F. Hourdin Modeling requirements for extending the maximum altitude of the Mars Climate model and database, *Technical Report, ESA 11369/95/NL/JG*, January 15, 1998.